Journal of Scientific & Industrial Research
Vol. 82, January 2023, pp. 75-85
DOI: 10.56042/jsir.v82i1.69947

Sustainable and Robust Techniques of Wireless Communications for Industry 4.0: Towards Efficient PAPR Reduction Models

Renuka Nellaturu

Department of ECE, RVR & JC college of Engineering, Guntur District 522 019, Andhra Pradesh, India

Received 13 June 2022; revised 02 October 2022; accepted 07 October 2022

This work presents the concerns of reliable, comprehensive, and high-quality communication networks essential in wireless communications for Industry 4.0. These are considered critical requirements of wireless technology for Industry 4.0. For a reliable transmission of digital data over broadband widths and Giga Hertz channels, the corresponding Peak-to-Average-Power Ratio (PAPR) must be under control. Industry standards Multiple-Input Multiple-Output Orthogonal Frequency Division Multiplexing With Offset Quadrature Amplitude Modulation (MIMO-OFDM/OQAM) system has been considered as the modulation technique with less Computational Complexity (CC). It usually produces phase sequence sets with different PAPR, a complex phenomenon to control. For robustness in PAPR control, the technique proposed has a receiver that initially restores the frequency domain rotation signal according to the sequence selection of the transmitter. Then it compares the distance between the reverse rotation sequence and the nearest constellation point to restore the original sequence. The proposed method simulation results can efficiently suppress the PAPR of MIMO-OFDM/OQAM signals. The proposed method is compared with the traditional Selective Mapping (SLM) algorithm. The proposed method reduces the CC, and can obtain the approximate Bit-Error Rate (BER) performance of the conventional SLM method when the sideband side information is known.

Keywords: Communication networks, Cyclic shift, MIMO-OFDM/OQAM, PAPR, SLM

Introduction

Unlike the first generation of the industrial revolution, Industry 4.0 refers to the convergence of several technologies, including sensing, communication, and big data processing. These are often termed the building blocks of Industry 4.0. Wireless communication has significantly been the functional part of handling large volumes of data during the digital manufacturing phase. This includes tracking the inventory of raw material through the manufacturing stages, digitalized warehouse management with high speed inter networking, distributing the data securely over long distances in less time, etc. In many cases, reliability is achieved through the quality of data transmission using complex modulation techniques for high security. Multiple in Multiple out systems are employed as the data must be disseminated to multiple nodes and vice versa. Several multiplexing-based modulation techniques are prominent for their efficiency in handling large data transmission volumes with quality. In this paper, advanced modulation techniques based on Orthogonal Frequency Division Multiplexing (OFDM) have improved their efficiency through suppression of Peak-to-Average Power Ratio (PAPR) issues.

Multiple-Input Multiple-Output OFDM with Offset-Quadrature Amplitude Modulation (MIMO-OFDM/OQAM) system uses frequency, time, and different antennas to obtain diversity gain, which can effectively resist multipath fading in wireless communications. Like OFDM/OQAM signals, MIMO-OFDM/OQAM is also a multi-carrier modulation signal. When the sub-carrier signals have the same phase or a slight difference, then the time-domain signals with larger amplitudes will be generated, resulting in PAPR. The transmitter of a communication system needs a wide linear range to transmit signals with a large PAPR. Transmitting signals beyond the linear range will produce non-linear distortion, resulting in decreased communication quality. It is essential to suppress PAPR of the MIMO-OFDM/OQAM signals. Commonly used methods to suppress PAPR include signal pre-distortion, coding, and selective mapping, partial transmission sequence.[1,2] Selective Mapping (SLM) and Partial Transmit Sequence (PTS) are the

Author for Correspondence
E-mail: renukanellaturu@gmail.com

most studied and effective methods.[3,4] The core idea of the traditional SLM algorithm (T-SLM) is to multiply the frequency domain signal by different phase rotation factors and then separately modulate it by the Inverse Fast Fourier Transform (IFFT) to obtain multiple time domain signals with different PAPRs, and then select the sequence with the smallest PAPR for transmission.

The joint Space-Frequency Blocks Coding (SFBC) and interleaved partitioning to reduce the number of IFFT operations, and generate more phase sequences through the exchange of block and parity parts.[5] Although this method can significantly reduce PAPR of the system, the parity transform brings additional sideband information. Literature proposed using SFBC coding and IFFT properties to reduce the CC through signal parity operations and cyclic shifts.[6] Literature proposed some improved low-complexity SLM algorithms.[7,8] The main idea is to divide the MIMO-OFDM/OQAM signal into multiple sub-blocks in the frequency domain to reduce the number of IFFT operations. As per the literature, each antenna separately uses different phase rotations to obtain multiple sequences, then perform IFFT modulation to obtain multiple time-domain signals, and then combines the time-domain signals in pairs to obtain more phase sequences.[9] The proposed based on time-domain cyclic shift Methods such as the exchange between antenna sub-blocks and other methods to generate multiple different PAPR phase sequences.[10,11] Although this method can effectively reduce the PAPR of system, the receiver needs to know which sub-blocks are exchanged at the transmitter to recover the original signal.

The Cyclic Shift SLM (CS-SLM) method is proposed in this work and is based on the signals time-domain cyclic shift and signal combination. The original signal is processed after the IFFT operation. To generate more phase sequences, only the cycle of signal is required. Shift, add and subtract signals between antennas. Taking 2 transmitting antennas as an example, the original frequency domain signal is subjected to IFFT modulation to obtain the time domain signal and then subjected to cyclic shifts of different lengths. The cyclic shift signals of different antennas are added and subtracted to obtain 2 new sequences, the cyclic shift sequence and the new sequence obtained by addition and subtraction forms a set of phase signals, in which any two sequences contain all the information of original signal, and the two sequences with the best PAPR performance can be selected for transmission. Therefore, in the method proposed in this paper, the transmitter only needs one IFFT operation and a small number of complex addition operations to obtain multiple sequence sets with different PAPRs, which reduces the CC; the receiver compares the reverse rotation sequence with its nearest signal constellation to restore the original signal by the distance of point, only the selection of signal in the phase set needs to be transmitted, and the sideband information is certain, and semi-blind detection is realized.

Methods and Techniques

If the number of transmit antennas in the MIMO-OFDM/OQAM system is N_t, the i-th transmit antenna frequency domain signal $X_i = [X_{0,i}, X_{1,i}, \ldots, X_{N-1,i}]$. The OFDM/OQAM system transmitted symbols are real-valued with time period of T. The complex OQAM signal $\{X_i = a_{2i} + ja_{2i+1}\}_{m\in N}$ is divided into real symbol vectors $\{a_i\}_{i\in N}$. In real values of OQAM symbols are staggering by $\frac{T}{2}$ duration of complex symbols $X_{k,i}$. Then, the obtained real symbols are undergone polyphase filtering of a prototype filter namely PHYDYAS filter.

$$x_i(n) = \sum_{m\in N}\sum_{k=0}^{LN-1} a_{k,m}\, g\left(n - m\frac{T}{2}\right) e^{j\left(\frac{2\pi kn}{T}+\phi_{k,m}\right)}{}_{\smile}X_i(k) \quad \ldots (1)$$

where, $g(t)$ is the prototype filter function with $L = 4T$ length and $\phi_{k,m} = \frac{\pi}{2}(k+m) - \pi km$. The discrete-time OFDM/OQAM symbols are given by

$$PAPR(x_i) = 10\, lg\, lg\left(\frac{(|x_i(n)|^2)}{E[|x_i(n)|^2]}\right) \quad \ldots (2)$$

where, $|x_i(n)|^2$ is the instantaneous power of signal, $max[\cdot]$ represents the peak power of signal, $E[\cdot]$ represents the average power of signal, and the PAPR of MIMO-OFDM/OQAM system is defined as

$$PAPR(x) = \{PAPR(x_1), \ldots, PAPR(x_{N_t})\} \quad \ldots (3)$$

Complementary cumulative distribution functions (CCDF) are generally used to indicate the probability that PAPR exceeds a threshold of $PAPR_0$

$$CCDF(PAPR(x)) = P_r(PAPR(x) > PAPR_0) \quad \ldots (4)$$

T-SLM Algorithm

Assume that the phase factor of T-SLM algorithm $P = [P_{i1}, P_{i2}, \ldots, P_{iK}]$ is multiplied by the k-th phase factor P_{ik} to obtain different phase sequences, where the phase factor $P_{ik} = [p_{ik}(0), p_{ik}(1), \dots, p_{ik}(N-1)]$.

$$X_{ik} = \sum_{n=0}^{N-1} p_{ik}(n) X_i(n) = P_{ik} X_i \quad \dots (5)$$

where, X_{ik} represents the signal that the original signal X_i multiplied by the phase factor P_{ik}. X_{ik} is modulated by IFFT to obtain an alternative time domain signal

$$x_{ik} = IFFT[X_{ik}] \quad \dots (6)$$

From the Fig. 1, it can be seen that when the T-SLM algorithm has K different phase factors P for each antenna, K different alternative sequences can be obtained. Calculate the PAPR of each phase sequence according to Eq. (2), denoted as $PAPR[x_{ik}]$, and then select the smallest one among the PAPR of K phase sequences as the PAPR of antenna, denoted as $PAPR[x_i]$

$$PAPR(x_i) = \{PAPR[x_{i1}], \dots, PAPR[x_{iK}]\} \quad \dots (7)$$

Choose a maximum of PAPR in all antennas as the PAPR of system

$$PAPR(x) = \{PAPR(x_1), \dots, PAPR(x_{N_t})\} \quad \dots (8)$$

In summary, in the T-SLM algorithm, each transmit antenna selects the sequence with the smallest PAPR from multiple phase sequences for transmission, so that the PAPR of MIMO-OFDM/OQAM system is suppressed. When the number of phase sequences is larger, the PAPR of MIMO-OFDM/OQAM system is more likely to be reduced, but each phase sequence needs IFFT modulation to obtain, the calculation complexity is higher, and the phase factor P is generally used as sideband sub-information transmission. When there are many sequences, more sideband information needs to be transmitted. The bit energy of sideband side information must be significantly higher than the signal energy to ensure its correct reception, reducing the system's frequency band utilization.

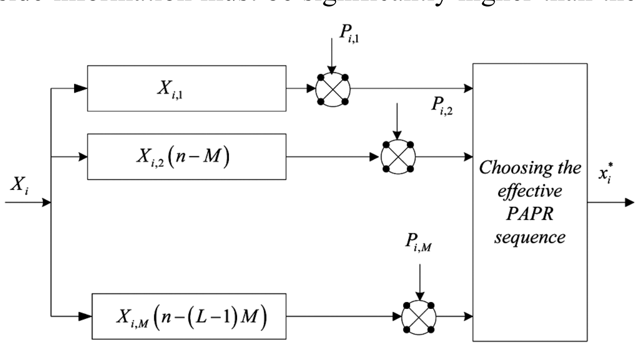

Fig. 1 — Traditional-SLM algorithm at transmitter

CS-SLM Algorithm

The basic idea of the CS-SLM algorithm proposed in this paper is at the transmitter, the original frequency domain signal of each antenna is directly passed through the IFFT module to obtain the time domain sequence, and the time domain sequence undergoes cyclic shift operations of different lengths before performing the inter-antenna signal conversion. Addition and subtraction operations, the sequence after each cyclic shift and the sequence obtained by addition and subtraction form a sequence set, each set selects 2 sequences with the best PAPR performance, and finally selects the best PAPR from all sets. The two sequences are transmission sequences; the received signal is restored to obtain the corresponding sequence at the receiver, according to the sequence specified in the transmitter set. Since the transmission signal undergoes a time-domain cyclic shift at the transmitter, the receiver should perform the corresponding frequency domain phase rotation on the signal, and calculate the distance from all frequency points of each rotating signal to the nearest signal constellation diagram, and select a minimum. The sequence corresponding to the distance is used as the original sequence, so as to realize the semi-blind detection of received signal.

A) CS-SLM Algorithm Transmitter

The MIMO-OFDM/OQAM signal X_i on the ith antenna is modulated by IFFT to obtain the time domain signal x_i, and the signal x_i is operated as follows

$$x(k) = \alpha_k(i) \sum_{i=1}^{N_t} a x_i \quad \dots (9)$$

where, $x(k)$ represents the new sequence obtained by the multi-antenna signal processing algorithm, the value of parameter a is $[0, \pm 1]$, and $\alpha_k(i)$ represents the power normalization factor. When $N_t = 2$, for a system with limited total power $\alpha_k(i) = \sqrt{1/8}$, this ensures that the total power of transmitted signal is consistent with the total power of original signal for a long period of time, while the power of a single antenna is limited, for the system, you need to choose a suitable $\alpha_k(i)$.[12] At this time, the algorithm in this paper can still be applied, but $\alpha_k(i)$ is no longer a constant, which is also the difficulty of a single power limited system. For a system with limited total power, a set of sequences can be obtained through Eq. (9),

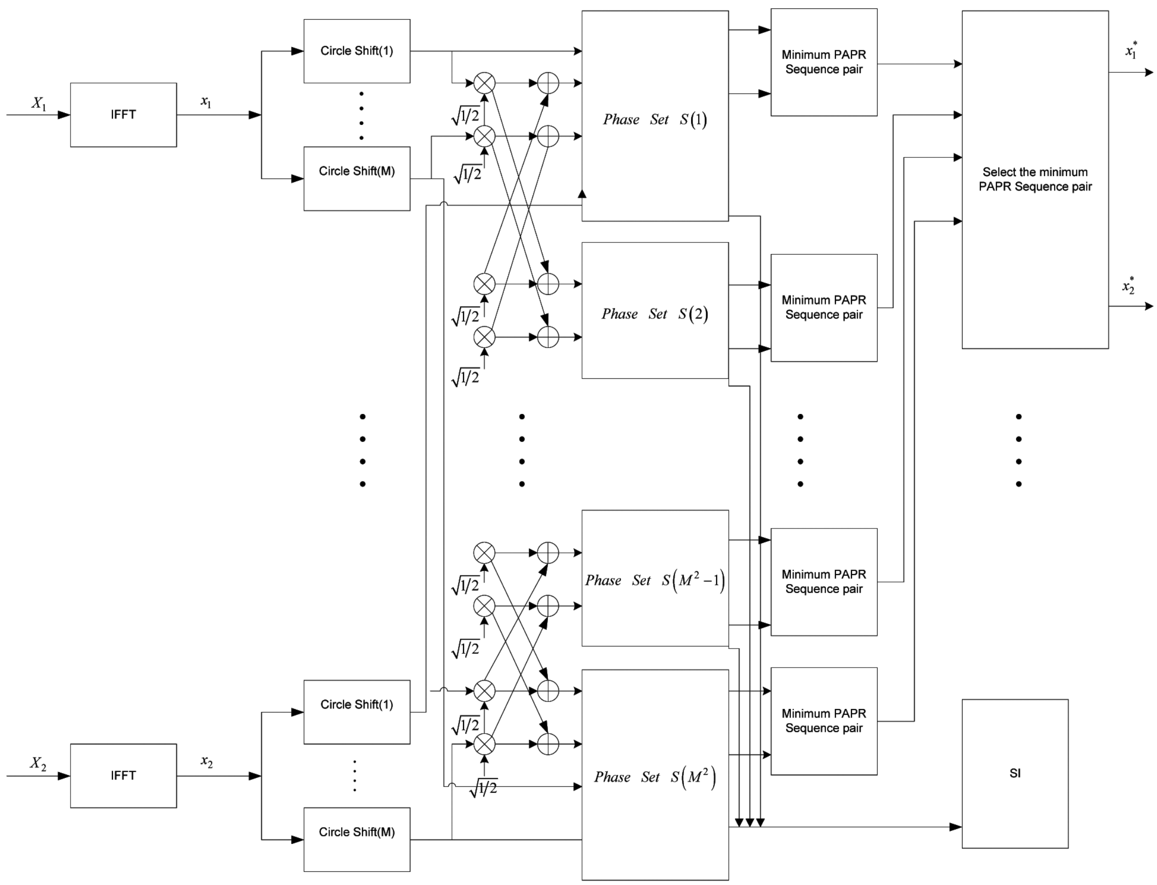

Fig. 2 — CS-SLM Algorithm

such as set $S(1)$, as shown in Fig. 2, without loss of generality. In the block diagram, $Circle\,shift(1)$ usually chooses cyclic shift the length is 0 (i.e., the original signal).

$$S(1) = \left[x_1 \frac{1}{2\sqrt{2}}(x_1 + x_2) x_2 \frac{1}{2\sqrt{2}}(x_1 - x_2)\right] \quad \ldots (10)$$

The four sequences of S(1) obviously have different PAPRs. It is worth noting that this article discards some other possible sequences in Eq. (9), such as $\left[x_1 \frac{1}{2\sqrt{2}}(x_1 + x_2) x_2 \frac{1}{2\sqrt{2}}(x_1 - x_2)\right]$, etc., These sequences have the same $PAPR$ as the four sequences given above. The four sequences in $S(1)$ can be combined in pairs to obtain $C_4^2 = 8$ groups of different combinations. The PAPR offset 8 combinations are calculated respectively, and the group with the smallest PAPR is selected as the phase transmission sequence for this set. Its $PAPR$ is marked as $PAPR[S(1)]$, and this selection is regarded as sideband information SI. The new sequence obtained by adding and subtracting the original sequence x_1 and x_2 in a particular transmission has a smaller peak value.[13] Therefore, selecting a new sequence can effectively reduce the PAPR of system, and its specific PAPR performance and analysis will be given in the simulation section.

In order to obtain more phase sequence sets with different PAPRs, the antenna signal x_i is subjected to more cyclic shifts of different lengths.[14] For the first antenna, assuming that the length of a certain cyclic shift is u_{12}, the shifted signal is expressed as

$$x_1(u_{12}) = circshift(x_1, [0, u_{12}]) \quad \ldots (11)$$

Shift the signal $x_1(u_{12})$ and the signal x_2 using Eq. (9) to get another set of alternative sequences

$$S(2) = \left[x_1(u_{12}) \frac{1}{2\sqrt{2}}(x_1(u_{12}) + x_2) x_2 \frac{1}{2\sqrt{2}}(x_1(u_{12}) - x_2)\right] \quad \ldots (12)$$

Since the circular shift of time domain signal does not change the PAPR of signal, the first sequence combination in $S(2)$ has the same PAPR as the sequence combination in $[x_1(u_{12}) \frac{1}{2\sqrt{2}}(x_1(u_{12}) + x_2)]$ with $S(1)$ and the sequence combination in

$\left[x_1 \frac{1}{2\sqrt{2}}(x_1+x_2)\right]$, so the sequence group in $S(2)$ is only $C_4^2 = 7$ different from $S(1)$.[15] With $S(1)$, you can get two alternate sequences with the minimum PAPR for $S(2)$ and the smallest PAPR for this set, which is recorded as PAPR $S(2)$.[16] Suppose that the circular shift length vector for the i root antenna signal is $U_i = [u_{i1}, u_{i2}, \dots, u_{iM}]$, where M is the number of circular shifts, passing Eq. (11) and pass-through Eq. (12), and a total of M^2 alternative sequence collections can be obtained, and the alternative collection is shown in Table 1.[(17)]

Calculate the minimum PAPR offset M^2 sets of sets, and select the smallest one as the optimal PAPR of algorithm

$$PAPR(S) = \{PAPR[S(1)], \dots, PAPR[S(M^2)]\} \quad \dots (13)$$

Select the two sequences with the best PAPR performance for STBC transmission in the set where the minimum PAPR is located, denoted as $[x_1^*, x_2^*]$, and reference gives the coding matrix.[18]

$$G = [x_1^* - (x_2^*)^H x_1^* (x_2^*)^H] \quad \dots (14)$$

where, $(.)^H$ represents the complex conjugate operation, the first OFDM/OQAM symbol period antennas one and two respectively send $[x_1^*, -(x_2^*)^H]$, the second OFDM/OQAM symbol period to send $[(x_2^*)^H x_1^*]$.[19]

The above is the PAPR suppression processing when $N_t = 2$ in the MIMO-OFDM/OQAM system. When $N_t = 3$, from Eq. (9) different sequences, such as $\left[x_1 x_2 \frac{1}{2\sqrt{3}}(x_1+x_2+x_3) x_3 \frac{1}{2\sqrt{3}}(x_1+x_2+x_3+x_4) \dots .\right]$ set, the signal of each antenna undergoes cyclic shifts of different lengths to obtain more phase sequence sets.

Table 1— Phase Sequence Set

PHASE	SEQUENCE SET
$S(1)$	$x_1 \frac{1}{2\sqrt{2}}(x_1+x_2) x_2 \sqrt{\frac{1}{2}}(x_1 x_2)$
$S(2)$	$x_1(u_{11}) \frac{1}{2\sqrt{2}}(x_1(u_{11})+x_2) x_2 \sqrt{\frac{1}{2}}(x_1(u_{11})-x_2)$
$S(M^2)$	$x_1(u_{1M}) \frac{1}{2\sqrt{2}}(x_1(u_{1M}) + x_2(u_{2M})) x_2(u_{2M}) \sqrt{\frac{1}{2}}(x_1(u_{11}) - x_2(u_{2M}))$

For the MIMO-OFDM/OQAM system with $N_t \geq 4$, it can be grouped, and the CS-SLM method with 2 or 3 antennas is used to reduce the PAPR of entire MIMO-OFDM/OQAM system by reducing the PAPR of antenna group. However, this expansion not all antennas are considered together. Still, the CS-SLM method proposed in this paper uses time-domain cyclic shift of signal and inter-antenna signal processing to generate more phase sequence sets, so each antenna group can get a good PAPR Performance, so that the PAPR of entire system can also be very suppressed.[20]

B) CS-SLM Algorithm at Receiver

It can be seen from Table 1 that the transmission signal is the best sequence of 2 PAPRs selected from a certain set $S(m)$.[21,22] Suppose a certain transmission sequence is the second sequence combination in $S(1)$

$$[x_1^* x_2^*] = \left[x_1 \frac{1}{2\sqrt{2}}(x_1+x_2)\right] \quad \dots (15)$$

The relationship between the transmitted signal and the original signal is

$$[x_1^* x_2^*] = [x_1 x_2] h(2) \quad \dots (16)$$

where, $h(2) = \left[10 \sqrt{\frac{1}{2}} \sqrt{\frac{1}{2}}\right]$, The signal $[x_1^* x_2^*]$ only needs to be multiplied by $[h(2)]^{-1}$ to get the signal $[x_1, x_2\ ]$. Analyzed by Eq. (10), except for $S(1)$, which has 6 combinations, other $S(m)$ has only 7 combinations.[23] Therefore, $S(1)$: $[h(l)\ 1 \leq l \leq 8]$, other$S(m)$: $[h(l)\ 1 \leq l \leq 7]$.

After the signal $[x_1^*, x_2^*]$ passes through the channel, the received signal first passes the FFT modulation module to obtain the frequency domain signal $[R_1, R_2]$, and the form of received signal can be expressed as

$$R_1 = H_{11} X_1^* + H_{12} X_2^* + N_1 R_2 = H_{21}(-X_2^*)^H + H_{22}(X_1^*)^H + N_2 \quad \dots (17)$$

where, $[X_1^* X_2^*]$ represents the frequency domain form of transmission signal $[x_1^* x_2^*]$, $H_{ij}(i, j\ 1, 2)$ expresses the transmission channel gain, $N_i(i\ 1, 2)$ which represents channel noise.[24] For signals with adjacent OFDM/OQAM symbol periods, there are generally: $H_{11} = H_{21} = H_1, H_{12}, H_{22} = H_2$, and the signal with original information $[Y_1, Y_2]$ can be solved by Eq. (17).

Analyzed by Eq. (15) and Eq. (16), the resolved signal $[Y_1 Y_2]$ must be multiplied by the combination of a transmitter antenna phase signal set $[h(l)]^{-1}$ to get the corresponding emission Signal form

$$[X_1^* X_2^*] = [Y_1 Y_2] h(l)^{-1} \qquad \dots (18)$$

where, $[X_1^*, X_2^*]$ represents the signal after the original frequency domain signal $[X_1, X_2]$ undergoes phase rotation. The specific steps of signal $[X_1^*, X_2^*]$ detection at the receiver are shown in Fig. 3, where, SI represents the sideband information of transmitter $[h(l)]^{-1}$.

In order to recover the original signal, it is necessary to know which cyclic shift factor u_{ik} was used. Generally, u_{ik} and $h(l)$ can be used together as sideband sub-information transmission, and the receiver can directly transmit the signal $[X_1^*, X_2^*]$ Perform reverse rotation to get the original signal. Blind detection method is proposed in this work to get the shift factor u_{ik}.[25] By the nature of FFT: the time domain cyclic shift of signal corresponds to the frequency domain phase rotation. As shown in Fig. 3, the frequency domain signal X_i^* is multiplied by different reverse rotation factors.

$$X'_{ik}(n) = X_i^*(n) e^{j2\pi u_{ik}(n-1)/LN} \qquad \dots (19)$$

where, $X'_{ik}(n)$ represents the i^{th} antenna signal $X'_i(n)$ when the shift factor $u_{ik}(u_{ik} \in U_i)$ rotates in the opposite direction, the signal value at the n^{th} frequency point is obtained.[26] Through the reverse phase rotation of frequency domain signal, M kinds of reverse rotation sequences can be obtained, in which there must be a reverse rotation sequence, and all of its frequency points have been rotated to the constellation point of modulation signal.[27] Due to the presence of noise, the inversion sequence may deviate from the original constellation point, but the sum of distances of all its frequency points from the nearest constellation point should be the smallest in probability. Therefore, first, determine each frequency point $X'_{ik}(n)$ of anti-rotation sequence as the nearest constellation point $X^Q(n)$, then calculate the sum of distances from all frequency points to $X^Q(n)$, and select the minimum. The u_{ik} corresponding to the distance is used as the shift factor used by the transmitting antenna, denoted as u'_i.

$$u'_i = min|X'_{ik}(n) - X^Q(n)|^2 \qquad \dots (20)$$

where, $X^Q(n) \in Q$ (Q is the signal constellation of the selected modulation method). The reverse rotation signal $X'_{ik}(n)$ corresponding to the shift factor u'_i is used as the restored original signal.

Complexity Analysis

Complexity Analysis at Transmitter

The number of subcarriers of OFDM/OQAM signal is N, and the over sampling rate is L, the number of complex multiplications and complex additions required for one IFFT operation are $LN/2lbLN$ and $LN\,lb\,LN$, respectively. When the number of phase sequences is K, the T-SLM algorithm requires K IFFT operations at LN points for each antenna to obtain K time-domain phase sequences.[28] The required complex multiplication and complex addition are $KLN/2\,lb\,LN$ and KLN respectively $lb\,LN$. This paper proposes the CS-SLM

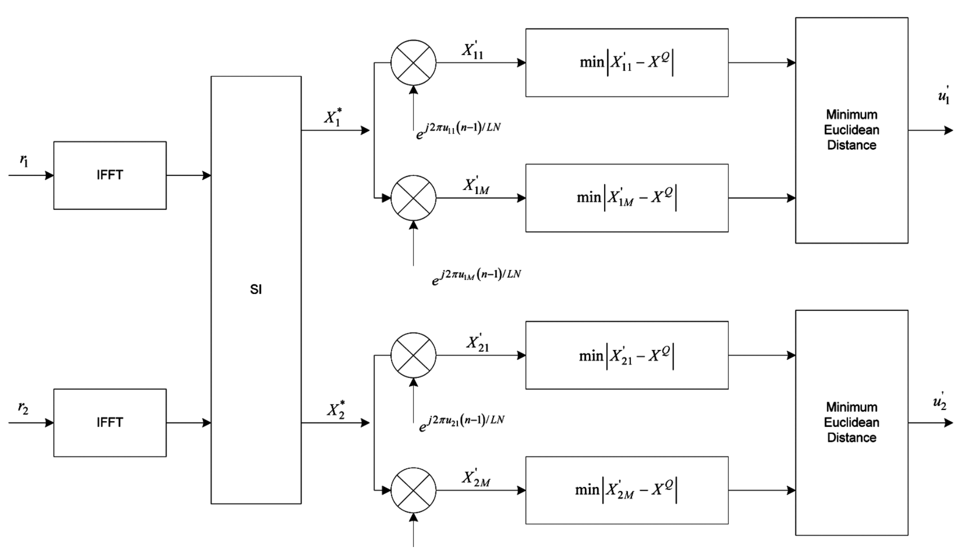

Fig. 3 — CS-SLM algorithm at receiver

algorithm. The original frequency domain signal only needs one IFFT operation to obtain the time domain signal. The required complex multiplication and complex addition are $LN/2\ lb\ LN$ and $LN\ lb\ LN$ respectively.[25–30] Cyclic shift and addition and subtraction operations to obtain multiple phase sequence sets, the required complex number addition is KLN (2 antennas require $2KLN$ complex number addition, the average of each antenna is KLN), the total number of complex multiplication and complex addition is $LN/2\ lb\ LN$ and $LN\ (lbLN + K)$.

For measuring the performance in terms of the computational complexity reduction ratio (CCRR) is defined as

$$CCRR = \left(1 - \frac{Complexity\ of\ CS-SLM}{Complexity\ of\ T-SLM}\right) \times 100 \quad \dots (21)$$

The computational complexity of each antenna is presented in Table 2 when the number of subcarriers is $N = 512$, the oversampling rate is $L = 4$, and the number of phase sets of T-SLM algorithm while the CS-SLM algorithm is K.

From the Table 2, it is compared with the T-SLM and CS-SLM algorithms. These both algorithms can greatly reduce the CC. When the number of phase sequences is 9 (the number of cyclic shifts M=2), the number of complex multiplications and complex additions required by CS-SLM is 90% and 80.8%, respectively, compared with T-SLM algorithm. It is worth noting that as the number of phase sequences increases, the ability of algorithm in this paper to reduce complexity will further increase. Therefore, the proposed CS-SLM algorithm has a greater advantage of reducing complexity.

Complexity Analysis at Receiver

The number of transmitting antennas is N_t and the number of phase sequences is K, the sideband side information that the T-SLM algorithm needs to transmit is $2lbK$ bits; the CS-SLM algorithm proposed in this paper requires $h(l)$ according to Eq. (18) (3 bit) this sideband sub-information is used to recover the rotation sequence. If the transmitter transmits the shift factor $u_i(lbK\ bit)$ as the sideband sub-information, the original signal can be recovered directly through Eq. (19), but this article CS-SLM proposes a blind detection method to restore u_i, as shown in Fig. 3.

Table 2 — Computational complexity of transmitter

Number of sets	Name	T-SLM	CS-SLM	CCRR
K=9(M=3)	Multiplications	92160	9210	90%
	Additions	192320	36912	80.8%
K=16(M=4)	Multiplications	163840	9840	93.9%
	Additions	327680	51248	84.36%

In T-SLM algorithm, the received signal requires an LN point FFT operation to obtain the frequency domain signal. Then according to the received sideband information, the frequency domain signal is directly multiplied by the corresponding phase factor to recover the original signal. Therefore, in the T-SLM method, the required complex number multiplication and complex number addition are $LN/2lbLNN$ and $LNlbLN$ respectively.

In the CS-SLM algorithm proposed in this work, the received signal also requires an LN point FFT operation to obtain the frequency domain signal, and then the sideband information is used to obtain the rotation signal according to Eq. (16). If u_i is known, the original signal is obtained by multiplying the reverse rotation factor directly according to Eq. (19). At this time, the complexity of receiver is equivalent to the T-SLM algorithm. If u_i is unknown, it requires M times of complex multiplication of LN points to realize the signal Inverse phase rotation. Similarly, M × N times of complex addition and M × N times of complex multiplication realize the distance between the anti-rotation sequence and the corresponding modulation signal constellation point to recover the shift factor. Therefore, the CS-SLM algorithm proposed in this paper needs a total of receiver The times of complex multiplication and complex addition are $LN/2lbLN + MN(L + 1)$ and $LNlbLN + MN$, respectively.

From the previous analysis, it can be seen that compared to the increase in the number of phase sequences at the transmitter as $M = 2$, the CC of receiver increases linearly with M. For example, when the number of cyclic shifts is $M = 3$ and $M = 4$, the number of phase sequence sets reaches 9 and 16, respectively. Therefore, the algorithm in this paper can achieve dynamic selection in terms of PAPR performance at the transmitter and receiver complexity. When the receiver complexity requirement is low, a smaller M can be selected so that the number of minimum distance calculations is less. At this time, the PAPR performance of system Decrease; on the contrary, you can choose a larger M to make the system have better PAPR performance.

Results and Discussion

Simulation results show that when the modulation mode is quadrature phase shift keying (QPSK), the number of subcarriers is 512, L=4, and the number of simulations is 10^7. Here, the CS-SLM algorithm selects different cyclic shifts. The impact and analysis of bit factor on PAPR performance, as well as the PAPR and bit error rate (BER) performance and analysis of typical algorithms.

Selection and Analysis of Cyclic Shift Factors

It is observed from Eq. (10) through Eq. (12) that when the shift factors of two antennas are the same, some sequence combinations in the set have the same PAPR, for example, when the cyclic shift factor of two antennas is $[0, u_2]$, the set of 2 phase sequences is obtained as follows

$$\{\left[x_1 \frac{1}{2\sqrt{2}}(x_1 + x_2)x_2 \frac{1}{2\sqrt{2}}(x_1 -)\right]\left[x_1(u_{12})\frac{1}{2\sqrt{2}}(x_1(u_{12}) + x_2(u_{12}))x_2(u_{12})\frac{1}{2\sqrt{2}}(x_1(u_{12}) - x_2(u_{12}))\right] \quad \ldots (22)$$

According to (22), the cyclic shift of same length of two antenna signals and the addition and subtraction operation can be written as the addition and subtraction of signal first and then the cyclic shift

$$\left[x_1(u_{12})\frac{1}{2\sqrt{2}}(x_1 + x_2)(u_{12})x_2(u_{12})\frac{1}{2\sqrt{2}}(x_1 - x_2)(u_{12})\right] \quad \ldots (23)$$

Obviously, the sequence in Eq. (23) and Eq. (22) has the same PAPR. Therefore, when the cyclic shift lengths of two antennas are the same, some sequence sets obtained by the combination have the same PAPR as the original sequence sets. Choosing such a cyclic shift factor becomes a calculation repetition. The Fig. 4 represents the PAPR performance of same and different U vectors.

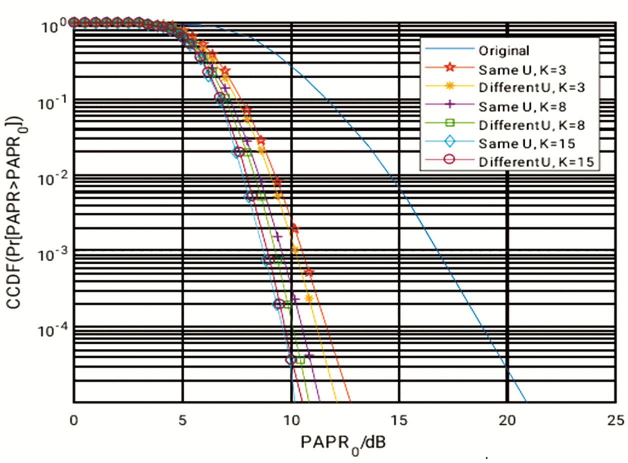

Fig. 4 — PAPR performance with same and different U

The same Figure represents the PAPR performance with different phase sequence sets and the same and different cyclic shift factors. When the number of phase sets is $K = 8$ (the number of cyclic shifts is $M = 5$), at 0.2% of CCDF, the PAPR of CS-SLM algorithm when the cyclic shift vector U is the same and different reaches 9.4 dB and 9.2 dB, respectively. The PAPR performance when the factor is different is about 0.2 dB better than when the shift factor is the same, which shows that choosing different U can effectively avoid calculation repetition and improve the PAPR suppression performance of algorithm.

PAPR Performance and Analysis of CS-SLM Algorithm

The PAPR performance curve presented in Fig. 5 corresponds to T-SLM algorithm and the proposed CS-SLM algorithm. When the phase sequence number is K = 8, T-SLM algorithm and CS-SLM algorithm can reduce the PAPR of the system effectively. At 0.2% of CCDF, the PAPR of CS-SLM algorithm and T-SLM algorithm are 9 dB and 8.8 dB, respectively. The CS-SLM algorithm is 0.3 dB worse than the T-SLM algorithm.

The reason for the above performance difference is that the T-SLM algorithm first operates in the frequency domain. The MIMO-OFDM/OQAM signal is multiplied by the different phase rotation factors and subjected to IFFT modulation to obtain multiple time-domain phase sequences with different PAPRs. The phase factors of T-SLM algorithm are statistically independent, and the new sequence obtained by multiplying with the original signal sequence is also independent. Its PAPR suppression performance is better, but the generated time-domain phase sequence requires IFFT operation. The CC is high. In this

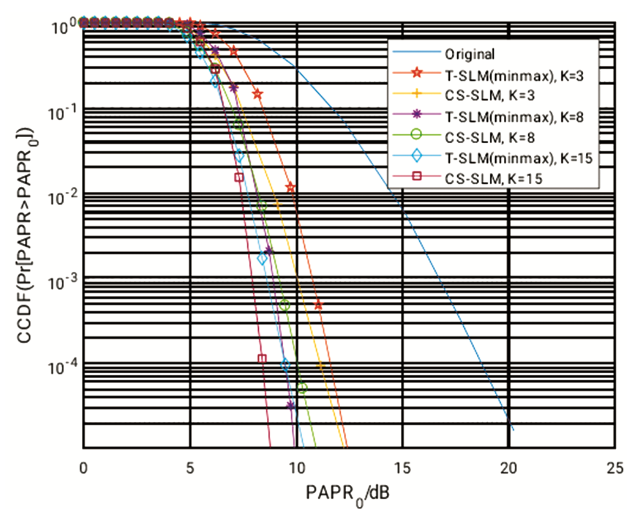

Fig. 5 — PAPR curve of T-SLM and CS-SLM

paper, the CS-SLM method is an IFFT operation to modulate the original frequency domain signal into the time domain and then use the cyclic shift of signal with different lengths and the addition and subtraction of signal between the antennas to obtain more phase signal sets. These signal sets have certain correlation between them, so the performance of reduced PAPR will be slightly worse than the T-SLM algorithm. However, the main advantage of this method is that only one IFFT operation is needed to add and subtract signals in the time domain. When the same number of phase sequences is generated, compared with the T-SLM algorithm, the CC is greatly reduced.

BER Performance and Analysis

In this paper, for verifying the BER performance the CS-SLM algorithm is proposed, this paper simulates the BER performance under two-channel models. Channel 1: Flat Rayleigh channel, where the channel gain H_i $(i = 1,2)$ is a complex Gaussian process with unity gain; Channel 2: EVA70 channel in LTE, its parameters: tap delay is 0 ns, 40 ns, 170 ns, 330 ns, 390 ns, 740 ns, 1100 ns, 1770 ns, 2570 ns, the corresponding tap power is 0 dB, −1.7 dB, −1.6dB, −3.8dB, −0.7dB, −9.8dB, −7.3 dB, −12.1 dB, −16.2 dB. N_i $(i = 1,2)$ is complex Gaussian noise. The simulation result is represented in Fig. 6.

It can be seen from Fig. 6 that the system BER performance curve of the semi-blind detection method proposed in this paper is consistent with the basic trend of BER performance curve of T-SLM algorithm with known sideband information. Taking channel 1 as an example, the BER performance of CS-SLM algorithm proposed in this paper is 2.3 dB worse than that of T-SLM algorithm. This is because it is assumed that the modulation method is QPSK, the power of each frequency point of T-SLM method signal is 1, and the proposed method in this work uses the addition and subtraction of signal. This operation makes the variance of transmission signal larger. Therefore, the BER performance of semi-blind detection method T-SLM proposed in this work is slightly worse at the receiver, but the sideband information required by the semi-blind detection method i.e., CS-SLM proposed in this work is certain, and does not increase with the increase of number of phase sequence sets, which effectively improves the efficiency of spectrum utilization.

The BER performance for different companding methods is illustrated in the Fig. 7, and in the Fig. 8 with HPA using QPSK and 16QAM modulation over

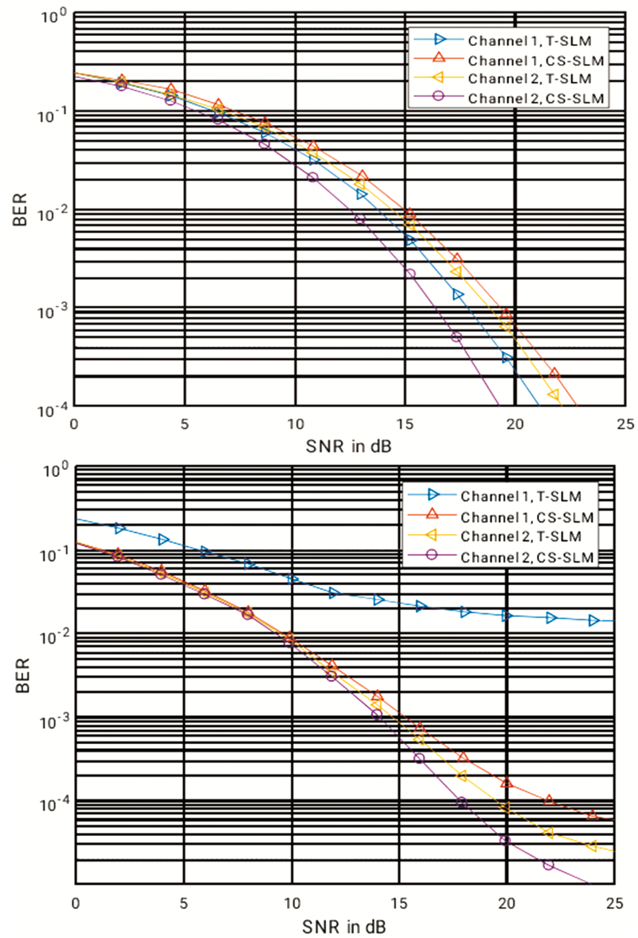

Fig. 6 — BER curves of T-SLM and CS-SLM with QPSK modulation under AWGN channel

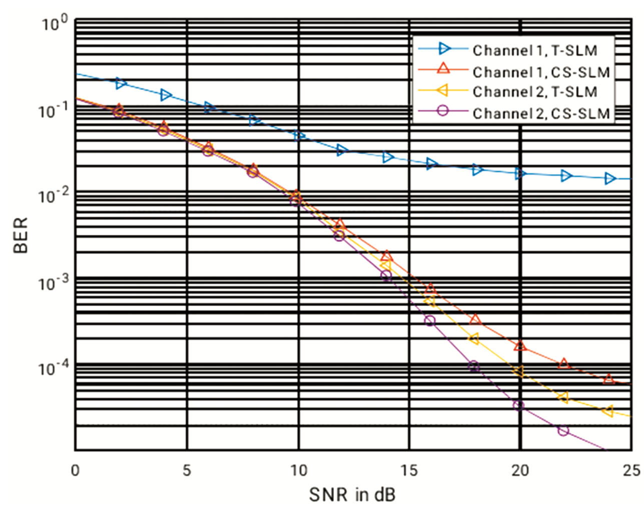

Fig. 7 — BER curves of T-SLM and CS-SLM with 16QAM modulation under AWGN channel

AWGN channel. It is observed from Fig. 7, that the algorithm can achieve low PAPR performance; the BER performance is further improved compared with

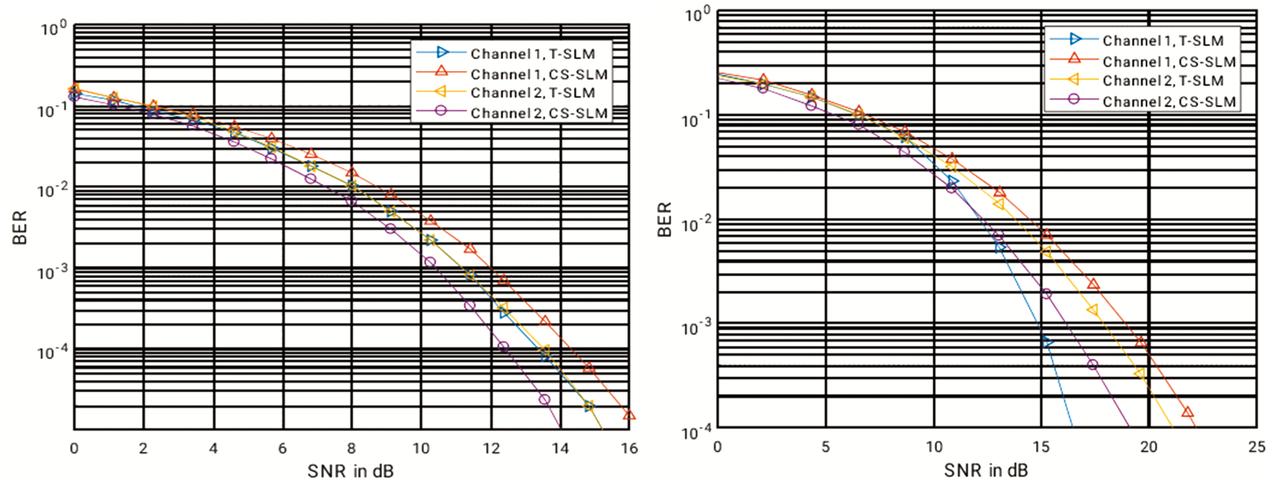

Fig. 8 — BER curves of T-SLM and CS-SLM with QPSK modulation with HPA over AWGN channel

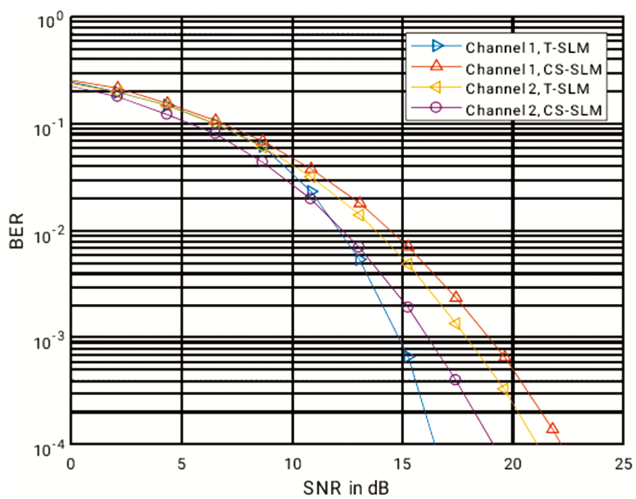

Fig. 9 — BER curves of T-SLM and CS-SLM with 16QAM modulation with HPA over AWGN channel

other T-SLM algorithms after the HPA model. The proposed algorithm is better than T-SLM over channel 1 and channel 2 with 2.05 dB and 1.2 dB respectively. It is illustrated in Fig. 8 that the performance is still better than other algorithms when using higher order modulations like 16 QAM modulation.

The BER performance curve of different SLM signals after two-path fading and AWGN channel in QPSK modulation mode is illustrated in Fig. 9. Since SLM introduces inter symbol interference, the receiver can get better without SLM and de-companding.

Conclusions

Reliable and sustained information exchange to meet the digital manufacturing requirements can be achieved through robust data transmission through complex modulation technique. The proposed modulation scheme has been implemented and demonstrated with empirical data. The performance analysis of the technique to suppress the PAPR and realize efficient and quality data transmission is presented. The analysis is carried out in terms of BER curves for T-SLM and CS-SLM. Multiple cyclic shift signals of 2 antennas are added and subtracted to obtain more for phase sequences with different PAPRs, each cyclic shift sequence and the new sequence obtained by the addition and subtraction operation form a signal set, and finally the sequence is selected with the smallest PAPR from multiple signal sets for transmission. Each antenna only needs one IFFT operation and signal addition and subtraction operations to obtain multiple sequence sets with different PAPRs, the CC is greatly reduced. At the receiver, sideband side information of sequence selection in the transmitter set is used to recover the rotation signal of each antenna, and then the reverse phase rotation signal is compared with the distance to the nearest constellation point to recover the original signal. Therefore, this method only needs a small amount of sideband side information to recover the original signal, which saves spectrum resources.

References

1 Kumar V S, PAPR Reduction Method for MIMO-OFDM/OQAM System Based on SFBC Structure, *Adv Intell Syst Comput* (2021) 607–615.

2 Mouna S, Fatma A & Mohamed S, Efficient embedded signaling through Alamouti STBC precoders in MIMO-OFDM systems, *IEEE Wirel Commun Netw Conf (WCNC)* (IEEE) 2013, 4053-4058.

3 Tan M, Zoran L & Yeheskel B N, STBC MIMO-OFDM peak-to-average power ratio reduction by cross-antenna

rotation and inversion, *IEEE Commun Lett*, **9(7)** (2005) 592–594.

4 Suban A, Brintha R R, Gayathri M, Prabha R N, Comprehensive analysis of MIMO-OFDM with PAPR reduction using PTS (The most efficient way of communication), *IEEE Students' Confn Electr Electron Comput Sci* (2012).

5 Tao J, Chunxing Ni & Lili G, A novel phase offset SLM scheme for PAPR reduction in Alamouti MIMO-OFDM systems without side information, *IEEE Signal Process Lett*, **20(4)** (2013) 383–386.

6 Su Y S, computationally efficient PAPR reduction of SFBC-OFDM signals by polyphase interleaving and inversion, *Intl Symp Wirel Pers Multimed Commun (WPMC)* 2014,

7 Ahmed A M & Erakkath A J, Adaptive modulation and interference cancellation techniques for MIMO-OFDM wireless networks, *Int J Netw Virtual Organ*, **18(3)** (2018) 246–264.

8 Renfors M, Mestre X, Kofidis E & Bader F, *MIMO-FBMC Receivers Orthogonal Waveforms and Filter Banks for Future Communication Systems* (Academic Press) 2017, 375–406, https://doi.org/10.1016/C2015-0-06484-X

9 Nikita G & Ahuja A K, Performance evaluation and comparison study of OFDM in AWGN and colored noise environment, in *Data Analytics and Management*, vol 54, edited by A Khanna, D Gupta, Z Pólkowski, S Bhattacharyya & O Castillo (Springer Nature Singapore Pte Ltd) 2021, 337–346.

10 Ouyang Y & Hungkai D, Peak-to-average power ratio reduction techniques for MIMO-OFDM systems with STBC/SFBC, *IEEE Int Conf Commun Problem-Solving (ICCP)* (IEEE) 2015.

11 Sandoval N & Francisco A, Peak to average power ratio reduction and error control in MIMO-OFDM HARQ System, *Diss École de techno supérieure*, (2019).

12 Li K, Sharan R R, Chen Y, Goldstein T, Cavallaro J R & Studer C, Decentralized baseband processing for massive MU-MIMO systems, *IEEE J Emerg Sel Topics Power Electron*, **7(4)** (2017) 491–507.

13 Geng J, Encoding and decoding schemes for MIMO system combined with convolutional code, *Appl Mech Mater*, **716** (2015) 1234–1238.

14 Yang, J, Pingzhi F, Trung Q D & Lei X, Exact performance of two-way AF relaying in Nakagami-m fading environment, *IEEE Trans Wirel Commun*, **10(3)** (2011) 980–987.

15 Alsharoa A, Ghazzai H, Kamal A E & Kadri A, Optimization of a power splitting protocol for two-way multiple energy harvesting relay system, *IEEE Trans Green Commun Netw*, **1(4)** (2017) 444–457.

16 Zhou M, Cui Q, Jantti R & Tao, Energy-efficient relay selection and power allocation for two-way relay channel with analog network coding, *IEEE Commun Lett*, **16(6)** (2012) 816–819.

17 Zhi-kang Z & Qi Z H U, Joint power allocation and multi-relay selection scheme based on system outage probability, *J China Univ Posts Telecommun*, **21(5)** (2014) 9–16.

18 Sun Y, Ng D W K, Ding Z & Schober R, Optimal joint power and subcarrier allocation for full-duplex multicarrier non-orthogonal multiple access systems, *IEEE Trans Commun*, **65 (3)** (2017) 1077–1091.

19 Gupta A, Singh K & Mathini S, Time-switching EH-based joint relay selection and resource allocation algorithms for multi-user multi-carrier AF relay networks, *IEEE Trans Green Commun Netw*, **3(2)** (2019) 505–522.

20 Gupta A & Mathini S, End-to-end learning-based amplify-and-forward relay networks using autoencoders, *IEEE Int Conf Commun (ICC)* (IEEE) 07–11 June, 2020.

21 Matsumine T, Toshiaki K A & Ye W, Deep learning-based constellation optimization for physical network coding in two-way relay networks, *IEEE Int Conf Commun (ICC)* (IEEE) 20–24 May 2019.

22 Hassan M Z, Hossain M J, Cheng J & Leung V C, Joint FSO fronthaul and millimeter-wave access link optimization in cloud small cell networks: A statistical-QoS aware approach, *IEEE Trans Commun*, **67(6)** (2019) 4208–4226.

23 Srivastava A & Rajeev R, Development of a fresh approach to use cooperative diversity for efficient & effective communication in modern wireless systems, *Int J Eng Techol*, **7(3)** (2018) 430–433.

24 Shi L, Cheng W, Ye Y, Zhang H & Hu R Q, Heterogeneous power-splitting based two-way DF relaying with non-linear energy harvesting, *IEEE Global Commun Conf* (*GLOBECOM*) (2018), 1–7.

25 Yulong Z, Zhu J & Xiao J, Joint power splitting and relay selection in energy-harvesting communications for IoT networks, *IEEE Internet Things J,* **7(1)** (2019) 584–597.

26 Amodu O A, Othman M, Noordin N K & Ahmad I, Relay-assisted D2D underlay cellular network analysis using stochastic geometry: Overview and future directions, *IEEE Access* **7** (2019) 115023–115051.

27 Shi H, Cai Y, Chen D, Hu J, Yang W & Yang W, Physical layer security in an untrusted energy harvesting relay network, *IEEE Access*, 7 (2019) 24819–24828.

28 Prathima A, Gurjar D S, Nguyen H H & Bhardwaj A, Performance analysis and optimization of bidirectional overlay cognitive radio networks with hybrid-SWIPT, *IEEE Trans Veh Technol*, **69(11)** (2020) 13467–13481.

29 Singh K, Ankit G & Tharmalingam R, QoS-driven resource allocation and EE-balancing for multiuser two-way amplify-and-forward relay networks, *IEEE Trans Wirel Commun*, **16(5)** (2017) 3189–3204.

30 Li X, Zhang Q, Zhang G & Qin J, Joint power allocation and subcarrier pairing for cooperative OFDM AF multi-relay networks, *IEEE Commun Lett*, **17(5)** (2013) 872–875.